Soft Matter

Accepted Manuscript

ROYAL SOCIETY OF CHEMISTRY

www.rsc.org/softmatter

Submitted to Soft Matter

Binding to semiflexible polymers: a novel method to control the structures of small numbers of building blocks

Dong Zhang[1], **Linxi Zhang**[2, *)]

[1]*Department of Physics, Zhejiang University, Hangzhou 310027, China*

[2]*Department of Physics, Wenzhou University, Wenzhou 325035, China*

Abstract

Through the molecular dynamics (MD) simulation method, it is found that long semi-flexible polymer chains can serve as an effective soft elastic medium to manipulate the ordered structures of small numbers of building blocks and the ordered structures of small numbers of building blocks can be easily controlled by chain bending stiffness. For two spherical particles in polymer-particle mixtures, three local organizations are identified: monomer level tight particle bridging, direct contact aggregation and dispersion. For small numbers of spherical particles in polymer-particle mixtures, the ordered structures of particles such as spherical and linear aggregations of particles depend mainly on chain bending stiffness. For non-spherical building blocks, the relative orientations of neighboring building blocks are also affected deeply by chain bending stiffness. This investigation can help us understand the complexity of the self-assembly of small numbers of building blocks in polymer-particle mixtures and the gene activity in living cells as well as construct novel materials in the nanotechnology field.

---

[*] Corresponding author. E-mail: lxzhang@zju.edu.cn.

1. Introduction

Over the past few years, the appearance of a spectacular variety of building blocks with different shapes, compositions, patterns and functionalities, which are enabled through chemical[1-4], physical[5-9] and biologically inspired[10-12] methods, has promised a potential future in the nanotechnology field[13]. The most concerned topic about the related issues is focusing on the construction of a set of universal strategies which can be used to control these building blocks to form the desired structures and then to realize the special functions. For the building blocks in bulk, the self-assembly under various modalities, including energy-driven, entropy-driven, templated and field-directed, holds the main key to discovering a novel nanomaterial with high performance[14-17]. In these cases, building blocks are strongly associated with each other and their intrinsic elements, such as shape, inter-block interaction and so on, dominate the final structures of the building blocks.

For a large number of building blocks, their main applications lie in the mixture with a polymer system (e.g., homogenous polymers, polymer mixtures and block copolymers)[18] and those mixtures are of major scientific and technological interest in diverse areas such as polymer science[19-20], nano-materials[21-23] and biology field[24]. The key issues about these polymer nanocomposites include spatial structure, particle dispersion, phase transition, gelation, and network formation, *etc*. Similarly, the self-assembly of building blocks in these polymer nanocomposites is still of importance, and both the above intrinsic building block elements (shape, inter-block interaction, etc.) and the extrinsic environment conditions[18] (the composition and molecular architectures of polymers, the interactions between building blocks and polymers, etc), will simultaneously play a key role in determining the final self-assembly structures of building blocks. For example, when low-volume fractions of nanorods are immersed in a binary, phase-separating blend, Balazs *et al.*[25] found that the cooperative effects of the fluid-fluid, fluid-rod and rod-rod interactions provide a means of manipulating the motion of nanoscopic objects and directing the rods to self-assemble into needlelike, percolating networks, while this supramolecular structure exhibits electrical or structural integrity.

For small numbers of building blocks (the number of building blocks roughly ranges from 1 to 100), the researches on the related issues may help us decipher the structure of matter at many different length scales[26], control the crystallization behaviors of particles[27], and understand the structure of chromatin[28]. For the case in which the direct inter-block attractive interaction is absent, the building blocks in the free status are nearly uncorrelated with each other when only small numbers of building blocks are present. Then, a suitable medium should be provided to collect these uncorrelated building blocks together and then to control their structures. Some existing experimental mediums used to study the packing of small numbers of spherical particles include liquid emulsion droplets[26] and aqueous solutions containing some small poly(Nisopropylacrylamide) (polyNIPAM) nanoparticles[29]. In this case, the structures of small numbers of building blocks mainly depend on the features of the added medium, and the intrinsic building block elements only play a secondary role. Therefore, for the purpose of well manipulation on the structures of small numbers of building blocks, it is necessary to provide some more suitable mediums. Inspired by some biological organizations, we suggest here that the soft elastic mediums, such as semiflexible polymer chain, fluid and elastic membranes, can be treated as a good medium to aggregate small numbers of building blocks together and to control the structures of these building blocks if the binding interaction between the soft elastic mediums and building blocks is present, and this assumption has been partially proved by some previous simulation works which focused on the spherical particles domain[30-32]. For instance, relying on the elastic property of membranes, the spherical particles adsorbed on planar fluid membranes can organize into ordered hexagonal arrays and branched linear aggregations[31], while the spherical particles adhering to the outer surface of an elastic nanotube can self-assemble into rings or helices and axial strings[32]. As expected, the structures of small numbers of building blocks binding to the soft elastic medium mainly depend on the topological and elastic properties of the medium.

In this paper, by employing molecular dynamics simulations, we show that long semiflexible polymer chain can serve as the illustrative soft elastic medium to control the structures of small numbers of binding building blocks. And both the spherical and non-spherical building blocks, such as particle, rod (1-dimension,1D), regular triangle and hexagon (2-dimension,2D) and regular tetrahedron (3-dimension,3D), are taken into account. By varying the elastic property of the soft medium, here referred to the stiffness of semiflexible polymer chains, the ordered structures of small numbers of building blocks can be easily controlled. Our results may be helpful to understand the gene activity in living cells and to construct novel materials in nanotechnologies.

2. Simulation methods

In our coarse-grained model, the long semiflexible polymer chain is modeled by *N* linked coarse-grained spherical monomers. To prevent overlap between any two monomers, a purely repulsive truncated and shifted Lennard-Jones potential is used

$$U_{LJ}(r)=\begin{cases}4\varepsilon\left[\left(\frac{\sigma}{r}\right)^{12}-\left(\frac{\sigma}{r}\right)^{6}+\frac{1}{4}\right], r\le 2^{1/6}\sigma\\ 0 \qquad\qquad\qquad\qquad\qquad , r>2^{1/6}\sigma\end{cases} \tag{1}$$

Where r is the distance between two monomers, σ is the monomer diameter, and $\varepsilon = k_B T$.

The neighboring monomers in polymers are linked by the finitely extendable nonlinear elastic (FENE) potential

$$U_{FENE}(r)=-\frac{KR_0^2}{2}\ln\left[1-\left(\frac{r}{R_0}\right)^2\right], r<R_0 \tag{2}$$

Here r is the distance between the two linked monomers, and the parameters are chosen to be $K = 30k_B T/\sigma^2$ and $R_0 = 1.5\sigma$.

The bending energy used to describe the stiffness of polymer chains is modeled by an angle potential between adjacent bonds

$$U_{bending} = b(1+\cos\theta) \tag{3}$$

Where θ is the angle between two consecutive bonds, and b is the bending energy. [33].

Volume exclusions between two spherical particles or between a particle and a monomer are imposed via shifted and truncated Lennard-Jones potentials of the expanded form[34]

$$U'_{LJ}(r)=\begin{cases}\infty \qquad\qquad\qquad\qquad\qquad , r\le\Delta\\ 4\varepsilon\left[\left(\frac{\sigma}{r-\Delta}\right)^{12}-\left(\frac{\sigma}{r-\Delta}\right)^{6}+\frac{1}{4}\right], \Delta<r\le\Delta+2^{1/6}\sigma\\ 0 \qquad\qquad\qquad\qquad\qquad , r>\Delta+2^{1/6}\sigma\end{cases} \tag{4}$$

The definition of $U'_{LJ}(r)=\infty$ for $r\le\Delta$ comes from the fact that the domain with $r\le\Delta$ is completely unreachable in MD simulations if the time step is sufficiently small. In fact, the LJ potential is exponentially increased when the distance r approaches gradually to Δ. For the particles with diameter $\sigma_p = 4\sigma$, the excluded interaction between two particles is described by $\varepsilon = k_B T$ and $\Delta = 3\sigma$, and the excluded interactions between particles and polymer monomers are described by $\varepsilon = k_B T$ and $\Delta = 1.5\sigma$.

The binding between particles and polymer monomers is achieved by employing a truncated Morse potential

$$U_{Morse}(r) = D_0\left[e^{-2\alpha(r-r_{mp})} - 2e^{-\alpha(r-r_{mp})}\right], r \le r_c \tag{5}$$

Here D_0 is the binding interaction, $r_{mp} = 2.5\sigma$ is the monomer-particle contact distance, and a soft parameter $\alpha = 1.25/\sigma$ and a long cut distance $r_{cut} = 10\sigma$ are used.

The non-spherical building blocks are constructed by N_c linked spherical particles and these particles are frozen into like rigid-like bodies through employing shifted Lennard-Jones potential introduced in eqn (1) with $\sigma = \sigma'$, FENE potential defined in eqn (2) with $R_0 = 1.5\sigma_p$, and the bending energy given in eqn (3) with $b = 10^4 k_B T$ for the neighboring particles. To describe the shape of building blocks well, a large overlap between the neighboring particles is allowed and $\sigma' = \sigma_p / 2$ is used. The excluded interactions between other nonadjacent particles are still described by eqn. (4) with $\varepsilon = k_B T$ and $\Delta = 3\sigma$. The interactions between two different building blocks or between building blocks and the polymer chains are realized by calculating all the related particle-to-particle or particle-to-monomer potentials given above. For rods, these particles are arranged into lines; for regular triangles and hexagons, these particles are arranged on a 2D hexagonal lattice; for regular tetrahedrons, these particles are arranged on a FCC lattice. The values of N_c for different building blocks are given in Table S1.

We use Molecular Dynamics to simulate the evolution of a NVT system in a $(500\sigma)^3$ periodic cubic box. The simulations are accomplished by performing Langevin dynamics with the open source software LAMMPS[35] at a reduced temperature $T^* = 1.2$. The friction coefficient $\gamma = 1/\tau_0$ and the time step $\Delta t = 0.01\tau_0$ ($\tau_0 = \sqrt{m\sigma^2/\varepsilon}$ is the time unit in our simulation) are used. In order to avoid the system from being locally trapped, after all building blocks have been adsorbed, a repeated slow reheat-annealing simulation process is employed until the targeted structures are sufficiently stable.

The polymer-mediated PMF can be calculated directly from simulations of two particles limit and is given by[34]

$$V(r_{pp}) = -k_B T \ln p_0(r_{pp}) \tag{6}$$

where $p_0(r_{pp})$ is the probability of finding particles separated by distance r_{pp} during simulations. To obtain $V(r_{pp})$ for a sufficient wide range of particle-particle separations, the umbrella sampling technique[36] is used, in which a series of biasing or window potentials $U_i^*(r_{pp}) = \frac{1}{2}k(r_{pp} - R_i)^2$ between the particles are used to force the particles to sample the full range of interparticle distances available in the simulation box. In our calculations, four umbrella sampling simulations are run at windows of $R_i = 4.0\sigma$, 5.0σ, 6.0σ, and 7.0σ. The parameter k is chosen to be $k = 4.0k_B T/\sigma^2$. This provides a set of interparticle distance histograms with sufficient overlap between the neighbor distributions. The weighted histogram analysis method[37] (WHAM) is used to obtain the unbiased probability distribution $p_0(r_{pp})$ from the umbrella sampling histograms.

3. Results and discussion

3.1 Two spherical particles limit

Here we only focus on the ability of the polymer stiffness in controlling the structures of small numbers of building blocks. To explore the effects of the polymer stiffness on controlling the local spatial organizations of building blocks and simultaneously to understand the physical picture of polymer-mediated inter-block interactions in the collection of small numbers of building blocks, the system of two spherical particles binding to semiflexible polymer chains is firstly considered. Here, "the local spatial organization" is employed to describe the spatial relative positions of two neighboring particles. As shown in Fig. 1(a), the average particle-particle distance $< d >$ as a function of bending energies at binding interaction $D_0 = 10k_BT$ directly indicates that there are three categories of polymer-particle organizations: monomer level tight particle bridging, direct contact aggregation and dispersion. For flexible chains (with bending energies $b \le 100k_BT$), the average particle-particle distance of $< d > \approx 5\sigma$ means that the two particles are bridging by one layer of polymer monomers. For semiflexible chains with a moderate stiffness of polymer ($b = 140k_BT$), the average particle-particle distance is very close to the size of particle ($< d > \approx 4\sigma$), which indicates that two particles in this case is direct contact aggregation. For rigid chains with bending energies $b \ge 240k_BT$, a large value of $< d >$ means that two particles are dispersed along rigid chains. The polymer-mediated particle-particle potentials of mean force (PMF) (see Fig. 1(b)) prove the above descriptions. The fact that the $V(r_{pp})$ reaches its minimum at $r_{pp}^{\min} \approx 5\sigma$ for the bending energies $b \le 100k_BT$ and gets its minimum at $r_{pp}^{\min} \approx 4\sigma$ for the moderate stiffness $b = 120 \sim 140k_BT$ means that the monomer level tight particle bridging and direct contact aggregation of particles are stable in their corresponding situations, while the PMF $V(r_{pp}) \approx 0$ at r_{pp}>4σ for rigid chain with $b = 300k_BT$ means that the two particles are almost unrelated to each other and this is the dispersion of particles. In a weaker ($D_0 = 5k_BT$) or a stronger ($D_0 = 15k_BT$) binding interaction, similar local spatial organizations of particles are also found. Some previous works about a pair of spherical particles dissolved in a completely flexible homopolymer melt (with bending energy $b = 0$) declare that there are three main categories of polymer-mediated organizations for particles: contact aggregation due to the depletion attraction for the athermal case, bridging at strong polymer-particle binding and steric stabilization for weak strength but long range attraction between particles and polymer.[38] Obviously, the organizations of two particles binding to semiflexible chains are different from those in flexible chains cases.

To get the physical details of polymer-mediated inter-block interactions in the collection of particles in a particle bridging or direct contact manner, the corresponding dynamic processes have been performed and one possible physical mechanism is illustrated in Fig. 2. For a sufficient binding interaction between particles and polymers, the adsorption of particles can lead to a large local deformation of polymer chains, and semiflexible chains can wrap the binding particles by several turns (Fig. 2(a)). A tight particle bridging can overlap the chain deformations and release some free polymer monomers, then drop the entropic losses (Fig. 2(b)). Kinetic effects may also contribute to this organization. For instance, wrapping of polymer chain around one binding particle for some turns will enhance the local polymer monomers density and then this local structure possesses some more odds to stabilize the another sliding particle[39] than other free polymer parts. Therefore, the combination of minimization of entropic losses with the kinetic effects leads to the formation of tight particle bridging for the flexible chain. In this case, the polymer-particle organization is dominated by the binding energy between particles and polymer chains. When the polymer stiffness increases, the bending energy of semiflexible polymer chains can affect the polymer-particle aggregations gradually. For the moderate chain stiffness, the contact aggregation of two particles can further decrease the chain deformations caused by the binding particles and simultaneously reduce the total polymer bending energy cost (Fig. 2(c)). Measurements of the related parameters, for example, the number of binding polymer monomers, the binding energy and the bending energy, at different simulation time for $b = 140k_BT$ are given in Fig. S1. The comparisons of the bending and binding energies between the bridging and the aggregating phases for the two-particle case are also made in Fig. S1. Therefore, we can conclude that the formation of the direct aggregation is driven by a decrease in both binding and bending energies. For the rigid chains, the binding particles can move freely along the completely stretched chains and the dispersion of particles is formed.

3.2 Small numbers of spherical particles and self-woven cage of chains.

Expectedly, the spatial arrangements of small numbers of spherical particles are affected by the polymer stiffness. Here, “the spatial arrangement” means mainly the spatial relative distribution of particles, which includes spherical or linear aggregation and dispersion. For flexible chains with bending energy $b = 0$, the structure of small numbers of particles is spherical packing in a dense manner to share the maximum of bridging monomers between neighboring particles and to minimize the binding energy in minimum entropy cost. Previous works[26] have indicated that the structures of microspheres in dense packing will mainly follow the minimal second moment of the mass distribution principle[40]. As shown in Fig. 3(a), when the number of particles ranges from $N_p = 4$ to $N_p = 13$, the one-to-one correspondence between our simulation results and the theoretical predictions shows that the structures of small numbers of particles for the complete flexible chains completely follow the minimal second moment of mass distribution principle. For a moderate polymer bending energy $b = 140k_BT$, the structures of small numbers of particles for different numbers of particles are arranged in a similar manner, the so-called linear contact aggregation, and a typical simulation result ($N_p = 8$) is given in Fig. 3(b). Considering the fact that the particle arrangement is controlled by the combination of particle-polymer binding energy and chain bending energy, the presence of this linear contact aggregation manner is easily comprehensible. On one hand, a semiflexible chain with a moderate bending energy can stretch into a linear structure, and then the particles binding to this polymer will also arrange in a linear manner. On the other hand, the semiflexible polymer-mediated inter-particle attraction caused by the deformation overlap mechanism will collect these binding particles in a direct contact manner to decrease the particle-polymer binding energy and the polymer bending energy simultaneously. Those two mentioned points will make the binding particles be aggregated in a linear contact manner for the moderate polymer bending energy. For a rigid chain with $b = 300k_BT$, the arrangements of small numbers of particles are dispersed along the stretched polymer chain (see Fig. 3(c)), which is consistent with the structure of two particles.

The spatial probability density distribution of pairs of particles is shown in Fig. 3(d). Here $P(r_{pp})$ means the probability density to find a pair of particles located in the distance interval $[r_{pp} - \Delta r_{pp}/2, r_{pp} + \Delta r_{pp}/2]$. For the flexible chain with $b = 0$, the first peak of $P(r_{pp})$ located at $r_{pp}^{1,peak} \approx 5\sigma$ means the neighboring pairs of particles are tightly bridging each other and $P(r_{pp}) = 0$ for $r_{pp} \geq 9.5\sigma$ indicates the particles are in spherical dense packing. For a moderate polymer stiffness $b = 140k_BT$, the first peak of $P(r_{pp})$ located at $r_{pp}^{1,peak} = 4\sigma$

means that the neighboring particles contact directly with each other and seven local sharp peaks on the profile of $P(r_{pp})$ in a distance interval $\Delta r_{pp} \approx 4\sigma$ clearly declares the arrangement of particles is in a linear contact manner. For the rigid chain, the particles are dispered along the ploymer chain and the value of $P(r_{pp})$ is relatvely small ($P(r_{pp}) \approx 0.01$) for $r_{pp} > 4\sigma$.

As shown in Fig. 4, the structures of small numbers of particles can also be described by shape factor $<\delta>$ and mean-square radius of gyration $<R_G^2>$ of particles. For the relatively flexible chains ($b < 80k_BT$), the particles are in spherical dense packing to minimize the second moment, and the shape factor is close to 0 ($<\delta> \approx 0.06$) and the mean-square radius of gyration reaches its minimum $<R_G^2> = 17\sigma^2$. When the polymer stiffness is increased, chain bending energy gradually affects the aggregation structures of particles. If the bending energies are increased further, the particles will be gradually dispersed and the shape factor will be slightly decreased, while $<R_G^2>$ is still rapidly increased. In conclusion, if the polymer bending energies are increased, the structures of small numbers of spherical particles experience a phase transition from spherical aggregation to linear contact aggregation until dispersion.

Generally speaking, our model can be regarded as a simple model of chromatin, in which a long semiflexible polymer chain represents a single duplex DNA chain and the particles represent nucleosomes, and the results presented here can help us well understand the gene activity in an eukaryotic cell. As we know, genes are silent in high-ordered structures such as the 30-nm chromatin fibers, and this is similar to the flexible polymer chain given here in which the particles are in dense packing. When genes are active in the open form of chromatin[41-42], nucleosomes will distribute along a single duplex DNA chain by being separated from each other by up to 80 bases pairs of linker DNA and it is usually referred to as a "beads-on-a-string" structure[43-46]. If the electrostatic interactions are taken into account in our model, the linear contact structure displayed for the moderate bending energy will present similarity with this beads-on-a-string structure. That is to say, the polymer-mediated PMF with moderate polymer stiffness will collect the particles in a linear contact manner, while the electrostatic repulsions between particles will prevent this collection, and the balance between the polymer-mediated PMF and the electrostatic repulsions will lead to the formation of this beads-on-a-string structure. Therefore, our results suggest the transition of genes from silent to active may be closely related to the effective bending energy of DNA, which is easy controlled by varying the salt concentration. Additionally, our results presented here are also consistent with a recent work about proteins binding by DNA, in which Brackley *et al.*[47] declared that, in the absence of any explicit interactions between proteins, or between templates, binding can induce spontaneously the local DNA compactions and protein aggregations.

The dynamic process of the formation of linear contact aggregation of particles with a moderate polymer stiffness (see Fig. S2) pronounces that semiflexible polymer chains can serve as a self-woven helical cage to collect particles in a linear contact manner. To discuss this self-woven helical cage in more detail, we slightly modify our model, in which a long polymer chain is replaced with a star semiflexible chain (Fig. S3). To form the concerned self-woven helical cage structure through using a linear polymer, a very long polymer is needed and this long polymer has to fold itself many times. However, if a star-polymer is used, the folding times of the polymers will be greatly reduced and it is of more energetically advantageous than using a linear polymer. The self-woven helical cage structure through using a star-polymer is more stable than using a linear polymer. Additionally, compared to using a linear polymer, when some more particles are added, the spontaneous adjustment of the self-woven helical cage structure in the star-polymer case is more convenient. As shown in Fig. S4, for the star semiflexible chain with a moderate polymer stiffness, the binding particles are aggregated in a linear contact manner to form a rod-like structure and the star chains helically wrap around this rod-like structure, just like a cage collecting the binding particles together. Here, the "self-woven" means the star chain weaves into a helical cage spontaneously and the length of the helical cage can be spontaneously varied to match the number of binding particles. As shown in Fig. 5, a short helical cage is observed for $N_p = 15$. When another five particles are added, the structure of the star polymer chain will spontaneously adjust and a new long helical cage is formed, whose length just matches the total number of binding particles. And the repeated operations can lead to the formation of a longer helical cage. This self-woven helical cage may be of potential application, such as the manipulation of particles into rod-like structures.

3.3 Shapes of building blocks.

Obviously, the effects of the polymer stiffness on the structures of small numbers of non-spherical building blocks are different from those of the spherical particles. Because of their anisotropic shapes, for non-spherical building blocks (such as rod, triangle, tetrahedron, etc.), apart from the local organizations (polymer bridging, direct contact and dispersion) and spatial arrangements (spherical and linear aggregation) mentioned above, the relative orientation of neighboring non-spherical building blocks will be also affected by the polymer bending energy. In general, this relative orientation of the neighbors can be analyzed using orientational correlation diagrams.[16] Here, for simplicity, we summarize the main correlations of the relative orientation as follows: for rods, they refer to side-to-side and end-to-end correlations; for regular triangles and hexagons, they include face-to-face and edge-to-edge correlations. For small number of one-dimensional building blocks, such as rods (see Fig. 6(a) top row), to minimize the particle-polymer binding energy at the minimum entropy cost, the sharing of the maximum of bridge monomers between any two neighboring rods in flexible polymer binding will result in the side-to-side parallel correlation. For the polymer with the moderate stiffness, under the effects of particle-polymer binding energy combined with polymer bending energy, the relative orientation of neighboring rods turns to be the end-to-end parallel correlation. For small numbers of two-dimensional building blocks, such as regular triangles (see Fig. 6(a) middle row) and hexagons (see Fig. 6(a) bottom row), to share the maximum of bridge monomers between two neighboring building blocks and then to reduce the entropic losses, the face-to-face parallel correlation of neighbors is firstly obtained in flexible chain binding. Under the effect of particle-polymer binding energy combined with polymer bending energy, the relative orientation of neighbors will turn to be the part edge-to-edge correlation (because of the absence of constraint on the rotation of polymer chains, such as, if the chain is chiral, the structures of these building blocks are expected to be also chiral) for the moderate polymer stiffness. For three-dimensional building blocks, such as regular tetrahedrons, the face-to-face correlation dominates the relative orientation of neighbors and the entropic "bonds" in the direction of the face normal are important.[16] For small numbers of regular tetrahedrons, the possible ordered networks of entropic "bonds" are diverse and their structure are more sensitive to polymer bending energy (see Fig.

S5).

For these non-spherical building blocks, such as rods, regular triangles and hexagons, in order to discuss the effects of polymer stiffness on the relative orientation of neighboring building blocks, an order parameter is defined as

$$< S >= \frac{1}{\sum_{i=1}^{N_b} N_{nb}^{i}} \sum_{i=1}^{N_b} \sum_{j=1}^{N_{nb}^{i}} \frac{3(\vec{a}_i \bullet \vec{e}_{ij})^2 - 1}{2} \tag{7}$$

Where N_b is the number of building blocks, N_{nb}^{i} is the number of neighboring building blocks for the *i*-th building blocks, $\vec{e}_{ij}$ is a unit vector pointing from the centroid of the *i*-th building block to the centroid of the *j*-th one. For rod, $\vec{a}_i$ is a unit vector parallel to the *i*-th rod; for regular triangles and hexagons, $\vec{a}_i$ is a unit vector perpendicular to the *i*-th building block. As shown in Fig. 6(b), for rods, $< S > \approx -0.5$ at $b \le 100 k_B T$ indicates the relative orientation of neighbor rods in the flexible polymer binding is side-to-side parallel correlation, while $< S > \approx 1.0$ at $b = 160 \sim 180 k_B T$ means the relative orientation of neighboring rods turns to be the end-to-end parallel correlation for the polymer with a moderate bending energy. The profile of the order parameter for rods experiencing an increase-to-decrease transition indicates that the relative orientation of neighboring rods is changed to be the end-to-end parallel correlation from the end-to-end parallel correlation and finally turns to be disordered when the polymer bending energies are increased. For regular triangles and hexagons, $< S > \approx 0.6$ at $b = 0$ means that, to a large extent, the relative orientation of neighboring building blocks is the face-to-face correlation for flexible chains. And $< S > \approx -0.5$ around $b = 250 k_B T$ means the relative orientation of neighbors are the edge-to-edge correlations for semiflexible chains with the moderate stiffness. The tendencies, firstly dropping and then rising, on the profiles of the order parameters for these two building blocks clearly denote the transition of the relative orientation of neighbors from the face-to-face correlation in the flexible polymer case to the edge-to-edge correlation for moderate polymer bending energy and finally to being disordered in the rigid polymer case. The local organizations and spatial arrangements as well as the relative orientation of non-spherical building blocks are affected by chain bending energies.

Conclusions

In this paper, through molecular dynamics computer simulations, we find that long semiflexible polymer chains can serve as an effective soft elastic medium to manipulate the structures of small numbers of building blocks when a sufficient strong binding interaction between polymer chains and building blocks is in presence. The effects of the polymer stiffness, which characterize the elastic property of semiflexible polymers, on controlling the structures of small numbers of building blocks are discussed in details through three aspects: the local organization of two neighboring building blocks, the spatial arrangement of centroid of small numbers of building blocks and the relative orientation of neighboring non-spherical building blocks. And the deformation overlap physical mechanism is given to explain the semiflexible polymer-mediated inter-block interaction in the aggregation of small numbers of building blocks. For the case of two spherical particles, three local spatial organizations are identified: monomer level tight particle bridging for flexible chains, contact aggregation for semiflexible chains with a moderate stiffness and dispersion for rigid chains. For small numbers of spherical particles, both the local organization and the spatial arrangement depend on the polymer stiffness, including the spherical dense packing which minimizes the second moment of the mass distribution in flexible chains binding, the linear contact aggregation for polymer with moderate stiffness and complete dispersion in rigid chains binding. For non-spherical building blocks, the local organization and the spatial arrangement as well as the relative orientation rely on the chain bending energies. These results indicate that the utilization of semiflexible polymer chains in controlling the structures of small numbers of building blocks is feasible and hierarchical, and this investigation can help us understand the gene activity in eukaryotic cells and construct novel materials in the nanotechnology field.

Acknowledgments

This research was financially supported by the National Natural Science Foundation of China (nos. 21374102, 21174131). **We are grateful to the reviewers of our manuscript for their detailed and insightful comments and suggestions.**

Supporting Information

Additional simulation results and a modified model.

References

1 N. R. Jana, L. Gearheart and C. J. Murphy, *J. Phys. Chem. B*, 2001, **105,** 4065–4067.

2 Y. G. Sun and Y. N. Xia, *Science*,2002, **298**, 2176–2179.

3 L. Manna, E. C. Scher and A. P. Alivisatos, *J. Am. Chem. Soc.*, 2000, **122**, 12700–12706.

4 R. C. Jin, Y. W. Cao, C. A. Mirkin, K. L. Kelly, G. C. Schatz and J. G. Zheng, *Science*, 2001, **294**, 1901–1903.

5 K. H. Roh, D. C. Martin and J. Lahann, *Nat. Mater.*, 2005, **4**, 759–763.

6 D. Dendukuri, D. C. Pregibon, J. Collins, T. A. Hatton and P. S. Doyle, *Nat. Mater.*, 2006, **5**, 365–369.

7 K. Braeckmans, S. C. De Smedt, M. Leblans, R. Pauwels and J. Demeester, *Nat. Rev. Drug Discov.*, 2002, **1**, 447–456.

8 Y. D. Yin, Y. Lu, B. Gates and Y. N. Xia, *J. Am. Chem. Soc.*, 2001, **123**, 8718–8729.

9 J. P. Rolland, B. W. Maynor, L. E. Euliss, A. E. Exner, G. M. Denison and J. M. De Simone, *J. Am. Chem. Soc.*, 2005, **127**, 10096–10100.

10 S. S. Shankar, A. Rai, B. Ankamwar, A. Singh, A. Ahmad and M. Sastry, *Nat. Mater.*, 2004, 3, 482–488.

11 V. Bansal, A. Sanyal, D. Rautaray, A. Ahmad and M. Sastry, *Adv. Mater.*, 2005, **17**, 889–892.

12 S. Brown, M. Sarikaya and E. Johnson, *J. Mol. Biol.*, 2000, **299**, 725–735.

13 S. C. Glotzer and M. J. Solomon, *Nat. Mater.*, 2007, **6**, 557–562.

14 B. A. Grzybowski, C. E. Wilmer, J. Kim, K. P. Browne and K. J. M. Bishop, *Soft Matter*, 2009, **5**, 1110-1128 and references therein.

15 A. Travesset *Science*, 2011, **334**, 183-184.

16 P. F. Damasceno, M. Engel and S. C. Glotzer, *Science*, 2012, **337**, 453-457.

17 A. F. Demirörs, P. P. Pillai, B. Kowalczyk and B. A. Grzybowski, *Nature*, 2013, **503**, 99-103.

18 L.-T. Yan and X.-M. Xie, *Prog. Polym. Sci.*, 2013, **38**, 369-405 and references therein.

19 G. Huber and T. A. Vilgis, *Macromolecules*, 2002, **35**, 9204-9210.

20 S. Vieweg, R. Unger, G. Heinrick and E. Donth, *J. Appl. Polym. Sci.*, 1999, **73**, 495-503.

21 B. J. Ash, L. S. Schadler and R. W. Siegel, *Mater. Lett.*, 2002, **55**, 83-87.

22 Y. Lin, A. Boker, J. He, K. Sill, H. Xiang, C. Abetz, X. Li, J. Wang, T. Emrick, S. Long, Q.

Want, A. Balazs and T. P. Russell, *Nature*, 2005, **434**, 55-59.

23 M. E. Mackay, T. T. Dao, A. Tuteja, D. L. Ho, B. Van Horn, H.-C. Kim and C. J. Hawker, *Nat. Mater.*, 2003, **2**, 762-766.

24 R. J. Ellise and A. P. Minton, *Nature*, 2003, **425**, 27-28.

25 G. Peng, F. Qiu, V. V. Ginzburg, D. Jasnow and A. C. Balazs, *Science*, 2000, **288**, 1802-1804.

26 V. N. Manoharan, M. T. Elsesser and D. J. Pine, *Science*, 2003, **301**, 483–487.

27 J. P. K. Doye, A. A. Louis, I-C. Lin, L. R. Allen, E. G. Noya, A. W. Wilber, H. C. Kok and R. Lyus, *Phys. Chem. Chem. Phys.*, 2007, **9**, 2197-2205.

28 A. A. Zinchenko, T. Sakaue, S. Araki, K. Yoshikawa and D. Baigl, *J. Phys. Chem. B*, 2007, **111**, 3019-3031.

29 G. Meng, N. Arkus, M. P. Brenner and V. N. Manoharan, *Science*, 2010, **327**, 560-563.

30 A. Šarić and A. Cacciuto, *Soft Matter*, 2013, **9**, 6677-6695 and references therein.

31 A. Šarić and A. Cacciuto, *Phys. Rev. Lett.*, 2012, **108**, 118101-1-5.

32 J. C. Pàmies, and A. Cacciuto, *Phys. Rev. Lett.*, 2011, **106**, 045702-1-4.

33 P. Cifra, *J. Chem. Phys.*, 2009, **131**, 224903-1-7.

34 D. Bedrov, G. D. Smith and J. S. Smith, *J. Chem. Phys.*, 2003, **119**, 10438-10447.

35 S. J. Plimpton, *J. Comput. Phys.*, 1995, **117**, 1-19.

36 G. M. Torrie and J. P. Valleau, *J. Comput. Phys.*, 1977, **23**, 187-199.

37 M. Souaille and B. Roux, *Comput. Phys. Commun.*, 2001, **135**, 40–57.

38 J. B. Hooper and K. S. Schweizer, *Macromolecules*, 2005, **38**, 8858-8869.

39 T. Sakaue, K. Yoshikawa, S. H. Yoshimura and K. Takeyasu, *Phys. Rev. Lett.*, 2001, **87**, 078105-1-4.

40 N. J. A. Sloane, R. H. Hardin, T. D. S. Duff and J. H. Conway, *Discrete Comput. Geom.*, 1995, **14**, 237-259.

41 B. Dorigo, T. Schalch, A. Kylangara, S. Duda, R. R. Schroeder and T. J. Richmond, *Science*, 2004, **306**, 1571-1573.

42 N. J. Francis, R. E. Kingston and C. L. Woodcock, *Science*, 2004, **306**, 1574-1577.

43 A. L. Olins and D. E. Olins, *Science*, 1974, **183**, 330-332.

44 F. Thoma, T. Koller and A. Klug, *J. Cell Biol.*, 1979, **83**, 403-427.

45 S. H. Leuba, G. Yang, C. Robert, B. Samori, K. van Holde, J. Zlatanova and C. Bustamante,

Proc. Natl. Acad. Sci. U.S.A., 1994, **91**, 11621-11625.

46 J. Bednar, R. A. Horowitz, J. Dubochet and C. L. Woodcock, *J. Cell Biol.*, 1995, **131**, 1365-1376.

47 C. A. Brackley, S. Taylor, A. Papantonis, P. R. Cook and D. Marenduzzo, *Proc. Natl. Acad. Sci. U.S.A.*, 2013, **110**, E3605-E3611.

Figure Captions

Fig. 1. (a) Average particle-particle distance $<d>$ as a function of bending energy b for various binding interactions D_0. Here the number of polymer monomers is N=500. (b) Polymer-mediated particle-particle potentials of mean forces (PMF) for various bending energies (b) at the binding interaction $D_0 = 10k_BT$. Here all the PMFs are shifted by $V(r_{pp} = 7\sigma) = 0$.

Fig. 2. Schematic illustrations show a possible physical picture of the aggregation process for two particles controlled by long semiflexible chains. (a) Semiflexible chains wrap around the binding particles by some turns at a strong binding interaction. (b) A tight particle bridging structure can overlap the deformations of semiflexible chains caused by two distant particles (labeled by the red color) and release some free chain monomers to minimize the entropic losses. (c) The contact aggregation of two particles can reduce the chain bending energy cost.

Fig. 3. Spatial arrangements of small numbers of spherical particles for various chain bending energies. (a) Spherical dense packing of bridging particles to minimize the second moment of the mass distribution at $b = 0$. Left and middle columns show the simulation snapshots for various particle numbers, and right column illustrates the corresponding theoretical results for a given number of particles (N_p). (b) Linear contact aggregation of particles at $b = 140k_BT$ and $N_p = 8$. (c) A dispersion distribution of particles along the stretched chains at $b = 300k_BT$ and $N_p = 8$. (d) Probability density distribution of pairs of particles with various chain bending energies and $N_p = 8$. Here $N = 1200$ and $D_0 = 10k_BT$.

Fig. 4. The shape factor $<\delta>$ (black square, left scale) and the mean-square radius of gyration $<R_G^2>$ (red circle, right scale) of particles as a function of chain bending energies at $N_p = 8$.

Fig. 5. A star semiflexible chain serves as a self-woven helical cage to collect particles in a linear contact manner, and inset figures show the rod-like structures with various numbers of particles. Here $b = 170 k_B T$

Fig. 6 (a) Ordered aggregation structures of non-spherical building blocks with different chain bending energies. (b) Order parameters $<S>$ as a function of chain bending energies for various building blocks.

Fig. 1(a)

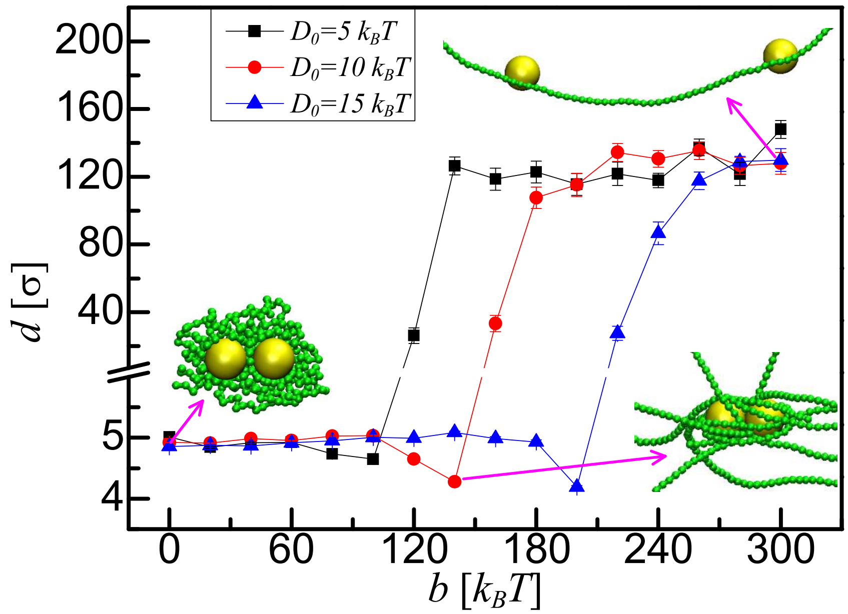
D_0=5 k_BT
D_0=10 k_BT
D_0=15 k_BT
200
160
120
80
40
5
4
d [σ]
0
60
120
180
240
300
b [k_BT]

Fig. 1(b)

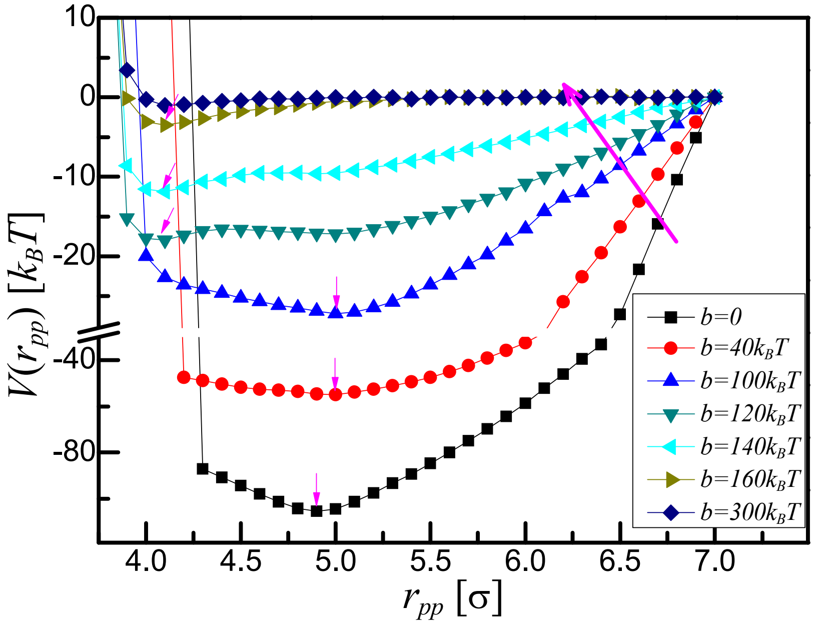
10
0
-10
-20
-40
-80
4.0
4.5
5.0
5.5
6.0
6.5
7.0
$V(r_{pp})$ $[k_BT]$
r_{pp} [σ]
b=0
b=40k_BT
b=100k_BT
b=120k_BT
b=140k_BT
b=160k_BT
b=300k_BT

Fig. 2

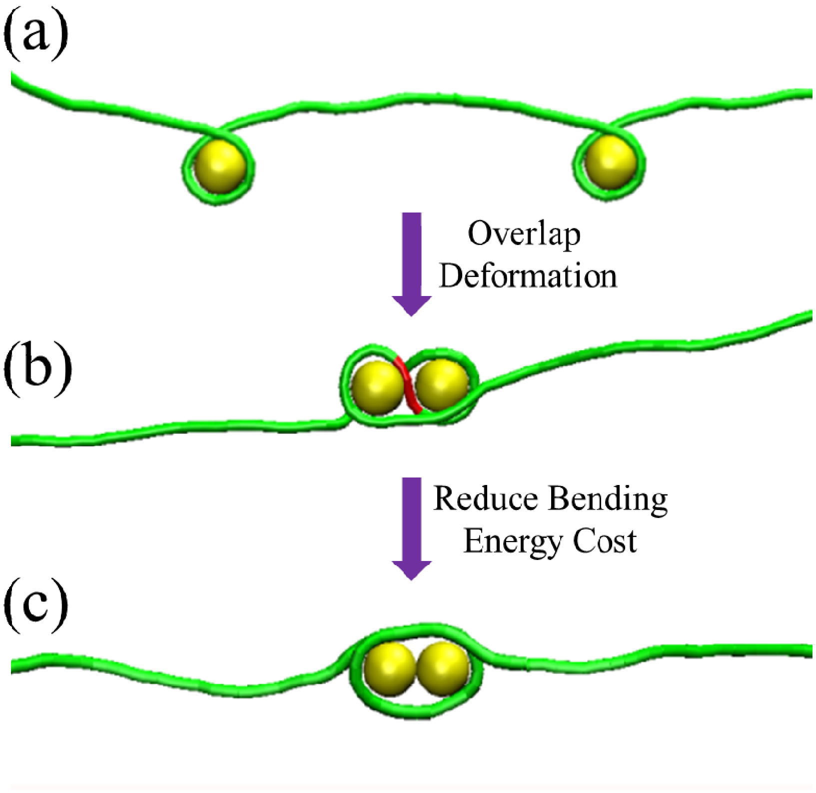

Fig. 3

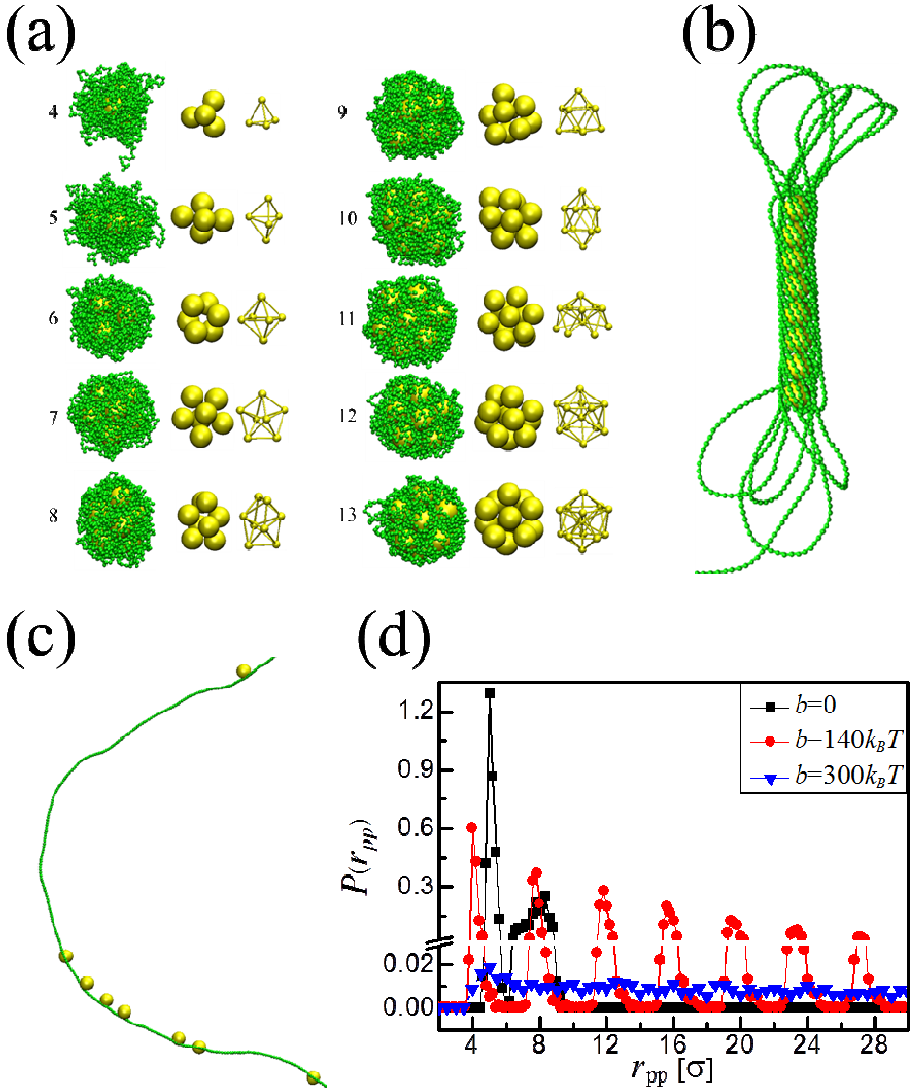
(a)
4
5
6
7
8
9
10
11
12
13
(b)
(c)
(d)
$P(r_{pp})$
1.2
0.9
0.6
0.3
0.02
0.00
4
8
12
16
20
24
28
r_{pp} [σ]
b=0
b=140k_BT
b=300k_BT

Fig. 4

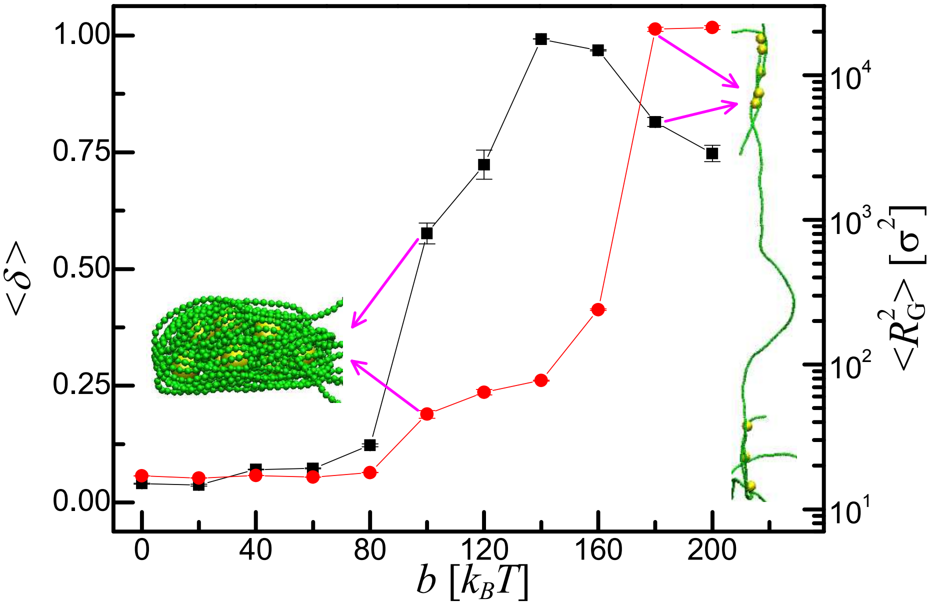
1.00
0.75
0.50
0.25
0.00
$<\delta>$
0
40
80
120
160
200
$b\ [k_BT]$
10^4
10^3
10^2
10^1
$<R_G^2>\ [\sigma^2]$

Fig. 5

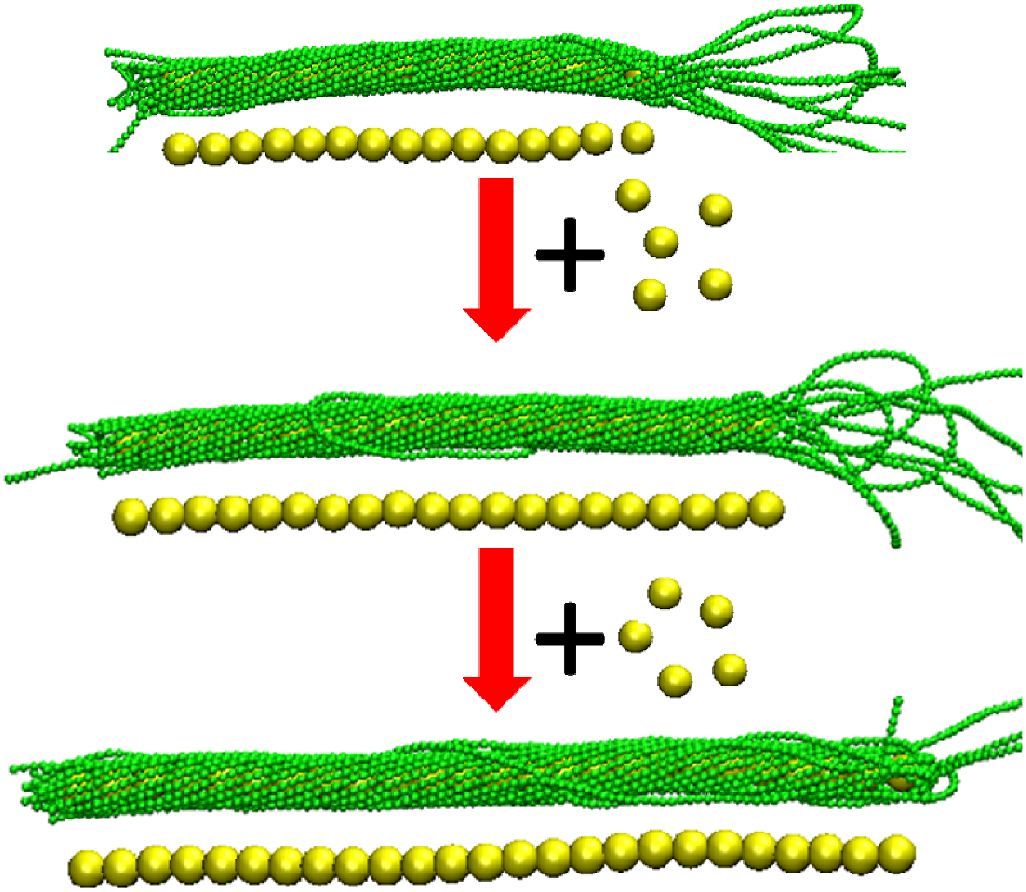

Fig. 6(a)

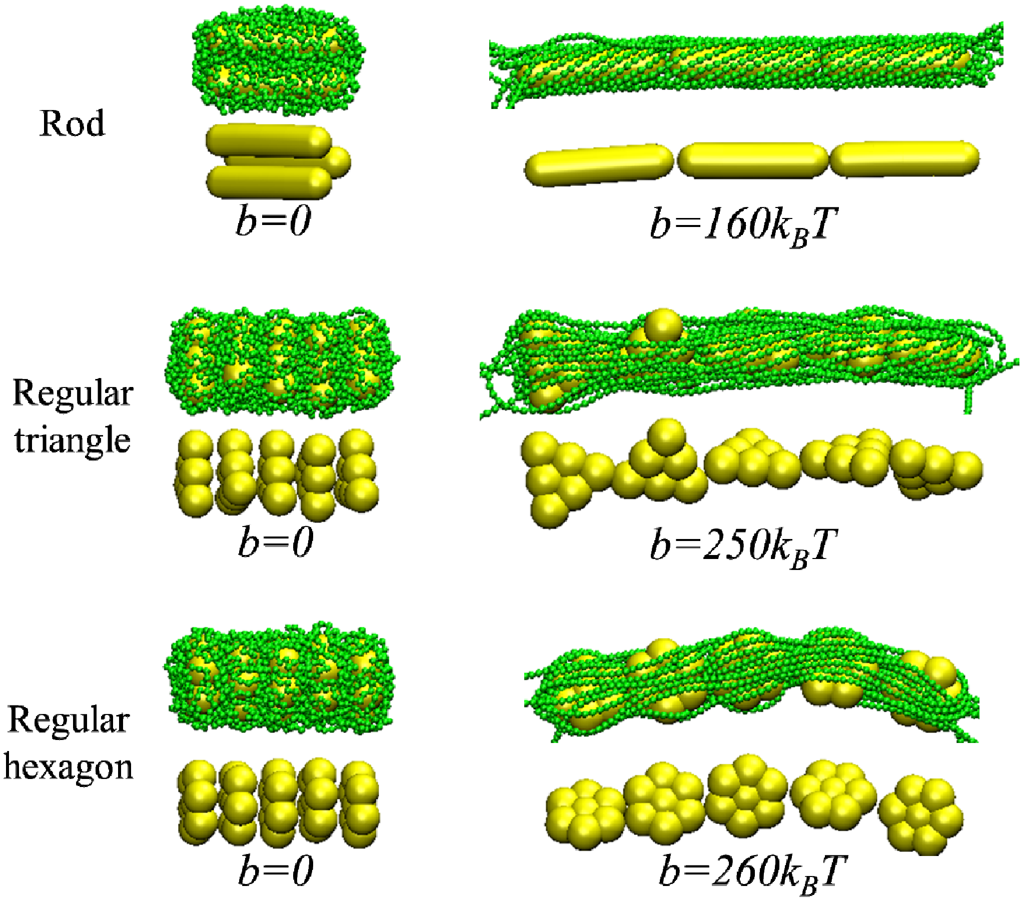
Rod
$b=0$
$b=160k_BT$
Regular triangle
$b=0$
$b=250k_BT$
Regular hexagon
$b=0$
$b=260k_BT$

Fig. 6(b)

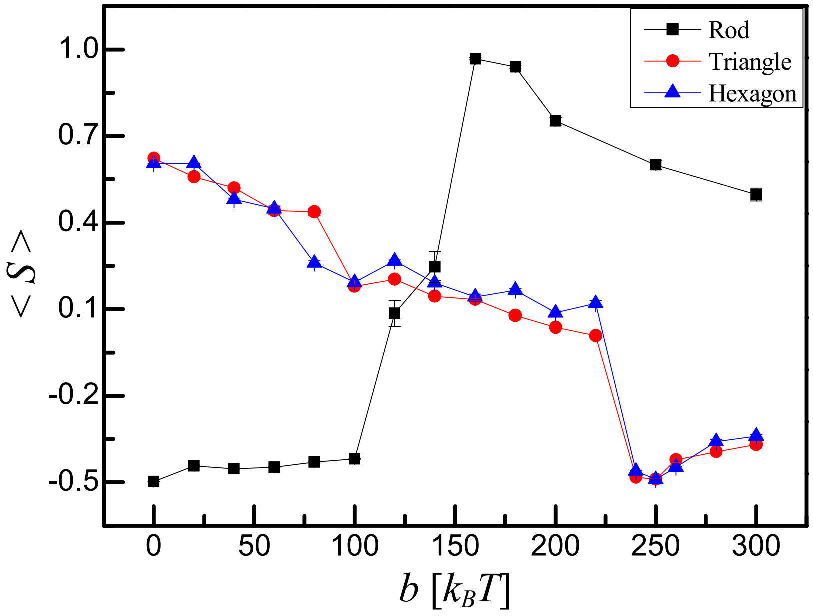
Rod
Triangle
Hexagon
1.0
0.7
0.4
0.1
-0.2
-0.5
$< S >$
0
50
100
150
200
250
300
$b\ [k_BT]$

Binding to semiflexible polymers: a novel method to control the structures of small numbers of building blocks

Dong Zhang, Linxi Zhang

Semiflexible polymer chains can serve as an effective soft elastic medium to control the structures of small numbers of building blocks through three different aspects: the local organization of two neighbor particles, the spatial arrangement of small numbers of building blocks and the relative orientation of neighbor non-spherical building blocks.